Acceleration and Loss of Relativistic Electrons During Small Geomagnetic Storms

B. R. Anderson,[1] R. M. Millan,[1] G. D. Reeves,[2,3] and R. H. W. Friedel[2,3]

Corresponding author: B. R. Anderson, Department of Physics and Astronomy, Dartmouth College, 6127 Wilder Laboratory, Hanover, NH 03755, USA (brett.r.anderson.gr@dartmouth.edu)

[1]Department of Physics and Astronomy, Dartmouth College, Hanover, New Hampshire, USA.

[2]Space Science and Applications, Los Alamos National Laboratory, Los Alamos, New Mexico, USA.

[3]The New Mexico Consortium, Los Alamos, New Mexico, USA.

Past studies of relativistic electrons have favored active storm-time periods, while the effects of small geomagnetic storms (Dst > -50nT) have not yet been statistically investigated. This is a timely study given the current weak solar cycle. We identify 342 small storms from a past solar cycle (1989-2000) and quantify the corresponding change in relativistic electron flux at geosynchronous orbit. Surprisingly, small storms can be equally as effective as large storms at enhancing and depleting fluxes. However, small storms are 10% less likely to result in flux enhancements and 10% more likely to result in flux depletions. All storms occurring during faster solar wind conditions are more likely to result in flux enhancements, but small storms tend to occur during periods of slower solar wind. Small geomagnetic storms clearly play a significant role in radiation belt dynamics and can provide new insights into the complex balance of acceleration and loss processes.

1. Introduction

It is well known that processes leading to radiation belt relativistic electron enhancements also lead to greater losses [e.g., *Turner et al.*, 2014]. Sometimes acceleration dominates and at other times loss, to either the magnetopause or atmosphere (precipitation), dominates. In fact, it is exactly this interplay between the various acceleration, loss, and transport mechanisms that brings about the wide range of observations in the radiation belts. Since the turn of the century, interest in the dynamic behavior of the radiation belts has grown immensely (for reviews, see *Millan and Baker* [2012], *Millan and Thorne* [2007], *Hudson et al.* [2008]). New missions, such as the Van Allen Probes, are making extraordinarily detailed measurements of the particle and wave environment throughout the radiation belts. Yet, solar cycle 24 has proven to be very weak, producing many fewer large geomagnetic disturbances than previous solar cycles.

In a precursor to this study, *Reeves et al.* [2003] statistically investigated the change of relativistic electron flux levels at geosynchronous due to moderate and large geomagnetic storms, those with minimum Disturbance Storm Time (Dst) index $<$ -50 nT [*Gonzalez et al.*, 1994]. (Hereafter, these storms will collectively be referred to as "large".) They found that large geomagnetic storms result in flux enhancements 53% of the time, no change to the flux level 28% of the time, and flux depletions 19% of the time. The size of the storm as measured by minimum Dst was determined to be a poor predictor of flux change. The only statistically significant correlation found was that storms occurring during higher solar wind speed conditions are more likely to result in flux increases than those occurring during slower solar wind conditions.

Small geomagnetic storms (minimum Dst > -50 nT) can also result in significant enhancement or depletion of radiation belt electrons. For example, on February 14, 2009 a small geomagnetic storm (minimum Dst was -36 nT) resulted in prolonged enhancement of relativistic electrons at geosynchronous orbit by several orders of magnitude (Figure 1). Concurrent with this small storm, electron precipitation was detected by a Balloon Array for Radiation-belt Relativistic Electron Losses [*Millan et al.*, 2013] payload located at the southern hemispheric magnetic foot point of the radiation belts. Including this event, all precipitation measured by BARREL has occurred during times when Dst was less negative than -53 nT.

Since different processes may be dominant during small storms compared with larger storms, it is therefore essential to understand the statistical response of relativistic electrons in the radiation belts to small geomagnetic storms as well. Here we extend previous analysis of electron response to storms to include smaller geomagnetic storms, to determine if, and how, investigating small events might lead to greater understanding of radiation belt dynamics.

2. Determining Changes in Relativistic Electron Flux

The method used in the present study closely follows *Reeves et al.* [2003] and analyzes the same period beginning in 1989 and ending in 2000. We begin by identifying small geomagnetic storms using one-hour resolution Dst data. The time of the storm is defined as the time of minimum Dst.

To identify the time of a small geomagnetic storm, we use an automated algorithm with three relatively simple criteria. The first criterion serves to select times for which Dst is

at a minimum value. The second criterion requires Dst be at least somewhat negative and restricts the identification to small geomagnetic storms only. The third and perhaps most crucial criterion requires a preceding sharp and significant drop in Dst, to avoid false identification of random and normal fluctuations in Dst. The criteria are summarized as:

1. Dst must be the first occurrence of the global minimum during a period extending 16 hours prior and 16 hours after.

2. Dst must be between -50 nT and -20 nT, inclusive.

3. Dst must decrease by at least 27 nT in the preceding 12 hours.

These criteria together select times for which Dst shows similar characteristics to large geomagnetic storms, namely a sharp drop in Dst indicating the start of the main phase followed by a recovery period extending several days or longer. Sometimes, a sudden storm commencement is indicated by a sharp rise in Dst prior to the drop. These criteria have been fine tuned to ensure random fluctuations in Dst do not trigger false identification of small storms while maximizing the identification of real storms. As a spot check, the list of identified small storms has been manually verified against hand-picked small storms for several randomly selected 1-year periods.

Further, we modified the criteria to similarly identify large geomagnetic storms, to allow for a direct comparison with results from *Reeves et al.* [2003]. The first criterion is the same. Obviously, the second criterion is changed to require Dst be less than -50 nT. The third criterion is changed to require a drop in Dst of at least 55 nT in the preceding 16 hours. Our automatic identification of large storms is in excellent ($> 80\%$ commonality) agreement with the storms identified by *Reeves et al.* [2003].

Figure 2 shows the Dst signature of all identified storms, small and large, for the two-week period centered on the time of storm, with the median and upper and lower quartile levels overlaid as black lines. For both sets of storms, there are occurrences when a given storm is closely preceded or followed by another storm, potentially affecting the results of this study. To asses the effect this may have, we create subgroups of "isolated" storms. These are storms that are separated temporally from any other storm, whether small or large, by at least 5 days.

To quantify the change in relativistic electron flux, we use LANL geosynchronous satellite 1.8-3.5 MeV electron flux data from the Energy Spectrometer for Particles (ESP) instrument [*Meier et al.*, 1996]. One-hour resolution data are weighted by each of the five satellite's lifetime average flux value and then averaged across all satellites at each time point, to create one consistent time series. We compare the 90th percentile highest flux value in the post-storm period (0.5-5.5 days after) to that of the pre-storm period (3.5-0.5 days before). The pre- and post-storm periods are defined to be consistent with previous studies and to account for diurnal variation in flux levels at geosynchronous. If the post/pre ratio is greater than 2, the storm resulted in an "increase" in relativistic electron flux. If the ratio is less than 0.5, the storm resulted in a decrease. Otherwise, the storm resulted in "no change".

For the following analysis, we also use solar wind velocity data from the OMNI database. We determine the maximum solar wind speed during each storm, as defined by 3.5 days prior to through 5.5 days after the time of minimum Dst. We compare the relativistic

electron flux enhancement or depletion for various maximum solar wind speed values as in *Reeves et al.* [2003].

3. Results

We identified 342 small geomagnetic storms between October 1989 and October 2000 for which geosynchronous LANL 1.8-3.5 MeV electron flux data were available. We similarly identified 234 large geomagnetic storms. In Figure 3 we plot the 90th percentile post-storm flux vs. pre-storm flux for all small and large storms. Each dot represents one storm. To guide the eye, each is colored as follows: red for "increase", green for "no change", and blue for "decrease". Note that the two plots are scaled identically. These two distributions are remarkably similar. This confirms two important observations from *Reeves et al.* [2003]. First, regardless of the size of the geomagnetic storm (as measured by Dst), a very wide range of geosynchronous relativistic electron responses are possible. Second, there is no correlation between pre- and post-storm flux levels, or in other words, any post-storm flux level can be preceded by any pre-storm level.

Of the 342 small geomagnetic storms, 144 storms (42%) resulted in relativistic electron flux enhancement at geosynchronous, 90 storms (26%) resulted in no-change, and 108 storms (32%) resulted in flux depletion. The large storms identified in this study showed the same proportions of flux increase/no-change/decrease as the large storms of *Reeves et al.* [2003], providing confidence in our analysis technique. These results are summarized in the top portion of Table 1. Comparing small storms to large storms, it is clear that small storms are less likely to produce an increase and more likely to produce a decrease in relativistic electron fluxes than large storms.

The first two plots in Figure 4 show the distribution of post/pre storm flux ratios for small and large storms. The third plot of Figure 4 shows cumulative function (CDF) curves for small (black) and large (red) storms. A CDF curve is here interpreted as the probability that a storm from a given subset of storms has a post/pre storm flux ratio less than a certain value. The largest difference between two CDF curves as well as the sample sizes of the two corresponding subsets can be used in a Kolmogorov-Smirnov test to determine the statistical likelihood that the difference between two curves is random. Here, the largest difference between the curves for all small storms and all large storms is 13%, as shown by the vertical black line in Figure 4, and the statistical likelihood that the difference between these curves is random is less than 2%.

To exclude possible effects from storms occurring in quick succession, we similarly analyzed the relativistic electron flux response to only the isolated storms. The results are much the same. (See bottom portion of Table 1.) Of the 91 isolated small storms, 33%/30%/37% resulted in enhancement/no-change/depletion of relativistic electron fluxes, respectively. Of the 71 isolated large storms, the corresponding proportions were 51%/23%/27%. The maximum difference between the two corresponding CDF curves (not shown, but similar to the third panel of Figure 4) increases to 22% and it remains unlikely ($< 3\%$) that this difference is random, despite the much smaller sample sizes. Thus the statistical difference we found for small versus large storms is confirmed when considering only isolated storms.

As shown by *Reeves et al.* [2003] for large storms, flux enhancements were correlated with periods of faster solar wind. We investigated whether a similar correlation would

hold true for small storms. Figure 5 shows cumulative probabilities for the post/pre flux ratio for small and large storms, each binned by maximum solar wind speed during the storm. The maximal difference between CDF curves for small storms is 43%, shown by the vertical black line, and the probability this is random is less than 0.004%. For large storms the maximal difference is only 31% and the probability of this being random is 2%, in excellent agreement with *Reeves et al.* [2003]. Thus, small storms show a stronger correlation between faster solar wind conditions and flux enhancements than do large storms.

As the tables within Figure 5 display, a much larger proportion of small storms occur during slower solar wind conditions than the same proportion of large storms. Concurrently, a much smaller proportion of small storms occur during faster solar wind conditions than large storms. The proportions of storms that occur during the middle ranges of solar wind speed conditions are comparable.

4. Discussion

We have examined the relativistic electron response at geosynchronous orbit for 342 small geomagnetic storms (minimum Dst > -50 nT) between October 1989 and October 2000. We have demonstrated that even though Dst remains above -50 nT, small storms have important effects on radiation belt relativistic electron fluxes. As a validation of our method, we identified 234 large storms during the same period and successfully reproduced the results of *Reeves et al.* [2003].

The effects on radiation belt relativistic electron fluxes of small geomagnetic storms are comparable with those of large storms, both in that the overall increase/no

change/decrease proportions are similar and that the flux enhancements and depletions can be equally as extreme. In confirmation of *Reeves et al.* [2003], post-storm fluxes show no correlation to pre-storm fluxes for any geomagnetic storm, regardless of size.

One might expect that with much less intense geomagnetic activity, radiation belt response would also be less, since many things do scale with Dst, for example number and intensity of injections, generation of waves, erosion of the plasmasphere, and radial diffusion. However, we find that the range of possible radiation belt responses does not scale with size of storm, even down to very small storms. This remarkable fact re-emphasizes the importance of carefully investigating the competing roles of acceleration and loss during any given storm, regardless of size.

Most intriguingly, however, there does exist a statistically significant difference between the distribution of flux changes for small and large storms. Compared with large storms, small storms are less likely to result in flux enhancements (42% vs. 52%) as well as more likely to result in flux depletions (32% vs. 22%). The proportions that result in no change in flux are the same. This result is confirmed even when we consider only those storms that occur more than five days before or after any other storm.

We have also shown that faster solar wind conditions increase the likelihood of a flux enhancement, regardless of size of storm, and that this correlation is much stronger for small storms than large storms. This, paired with the fact that small storms are more likely to occur during slower solar wind conditions, just as large storms are more likely to occur during faster solar wind conditions, is consistent with the difference between the distribution of flux changes for small and large storms.

What causes the interplay between physical processes to balance differently for small versus large storms? It seems reasonable that smaller storms experience sustained acceleration less often. Larger storms are perhaps more likely to be driven by co-rotating interaction regions. But why would smaller storms also experience greater losses more often? One explanation might be that small storms tend to be driven by coronal mass ejections, which do not necessarily require high solar wind velocity, but which do compress the magnetosphere upon impact, causing more intense losses to the magnetopause. Our study focuses only on geosynchronous electrons, which may be more immediately susceptible to magnetopause shadowing than electrons deeper in the radiation belts.

This study also shows yet again that Dst is a poor predictor of relativistic electron dynamics in the radiation belts. Dst, as a measure of ring-current energy density, is dominantly influenced by ions. The processes that lead to relativistic electron acceleration, loss, and transport depend heavily on the electron source population and waves, some of which depend also on electrons (e.g. chorus waves depend on KeV electrons). Yet these populations contribute very little to Dst. Certainly, geomagnetic storms often do cause drastic electron flux changes; nevertheless, ring current dynamics and relativistic electron flux dynamics are somewhat decoupled.

To further answer these questions, investigations into numerous individual events, including small storms, will be required. This study could also be expanded into the recent solar cycle to include times after the launch of the Van Allen Probes. Newly acquired Van Allen Probe data, in combination with other satellite and ground-based (e.g. balloon) data sets, make possible deeper investigations into individual storms as well as more

comprehensive statistical analysis. The contribution from electrons and ions to the ring current energy density could be explored using the same data sets.

That small storms play a large role in radiation belt dynamics becomes even more significant in light of the relatively quiet geomagnetic conditions of the current solar cycle. Our storm finding algorithm applied to January 2009 (roughly solar minimum) through April 2015 identifies 64% fewer large storms (42) than the corresponding period following the previous solar minimum in 1996 (117). Small storms, by definition, occur in quieter periods of geomagnetic activity. This may actually allow for more clear analysis of cause and effect relationships in radiation belt dynamics. Small storms, therefore, provide important opportunities to study the radiation belts. In the midst of the current weak solar cycle, this is an encouraging fact.

Acknowledgments. This research was supported in part by the Balloon Array for Radiation-belt Relativistic Electron Losses (BARREL) NASA grant NNX08AM58G. B.A. thanks the New Hampshire Space Grant Consortium for graduate support as well as Alexa Halford, Michael McCarthy, and Leslie Woodger for numerous conversations that enhanced the present study. The authors thank the World Data Center for Geomagnetism, Kyoto and the Hermanus, Honolulu, Kakioka, San Juan, and INTERMAGNET observatories for providing the Dst index. We thank the Goddard Space Flight Center Space Physics Data Facility for use of their OMNIWeb Plus service to access OMNI data and CDAWeb service to access NOAA GOES data. Data from the LANL-GEO SOPA instrument were provided by the US Department of Energy's Los Alamos National Laboratories and are available upon request from Geoff Reeves (reeves@lanl.gov).

References

Gonzalez, W. D., J. A. Joselyn, Y. Kamide, H. W. Kroehl, G. Rostoker, B. T. Tsurutani, and V. M. Vasyliunas (1994), What is a geomagnetic storm?, *Journal of Geophysical Research (ISSN 0148-0227)*, *99*, 5771, doi:10.1029/93JA02867.

Hudson, M. K., B. T. Kress, H.-R. Mueller, J. A. Zastrow, and J. B. Blake (2008), Relationship of the van allen radiation belts to solar wind drivers, *Journal of Atmospheric and Solar-Terrestrial Physics*, *70*, 708, doi:10.1016/j.jastp.2007.11.003.

Meier, M. M., R. D. Belian, T. E. Cayton, R. A. Christensen, B. Garcia, K. M. Grace, J. C. Ingraham, J. G. Laros, and G. D. Reeves (1996), The energy spectrometer for particles (esp): Instrument description and orbital performance, *Workshop on the Earth's trapped particle environment. AIP Conference Proceedings*, *383*, 203, doi:10.1063/1.51533, 1996: American Institute of Physics.

Millan, R. M., and D. N. Baker (2012), Acceleration of particles to high energies in earth's radiation belts, *Space Science Reviews*, *173*, 103, doi:10.1007/s11214-012-9941-x, (c) 2012: The Author(s).

Millan, R. M., and R. M. Thorne (2007), Review of radiation belt relativistic electron losses, *Journal of Atmospheric and Solar-Terrestrial Physics*, *69*, 362, doi:10.1016/j.jastp.2006.06.019.

Millan, R. M., M. P. McCarthy, J. G. Sample, D. M. Smith, L. D. Thompson, D. G. McGaw, L. A. Woodger, J. G. Hewitt, M. D. Comess, K. B. Yando, A. X. Liang, B. R. Anderson, N. R. Knezek, W. Z. Rexroad, J. M. Scheiman, G. S. Bowers, A. J. Halford, A. B. Collier, M. A. Clilverd, R. P. Lin, and M. K. Hudson (2013), The balloon array for

Table 1. Results of Small and Large Storm Relativistic Electron Response

	342 Small Storms	234 Large Storms
Flux Increase	144 (42%)	121 (52%)
No Change in Flux	90 (26%)	61 (26%)
Flux Decrease	108 (32%)	52 (22%)

	91 Isolated Small Storms	71 Isolated Large Storms
Flux Increase	30 (33%)	36 (51%)
No Change in Flux	27 (30%)	16 (23%)
Flux Decrease	34 (37%)	19 (27%)

rbsp relativistic electron losses (barrel), *Space Sci. Rev.*, *179*, 503, doi:10.1007/s11214-013-9971-z, (c) 2013: The Author(s).

Reeves, G. D., K. L. McAdams, R. H. W. Friedel, and T. P. O'Brien (2003), Acceleration and loss of relativistic electrons during geomagnetic storms, *Geophys. Res. Lett.*, *30*(10), 1529.

Turner, D. L., V. Angelopoulos, W. Li, J. Bortnik, B. Ni, Q. Ma, R. M. Thorne, S. K. Morley, M. G. Henderson, G. D. Reeves, M. Usanova, I. R. Mann, S. G. Claudepierre, J. B. Blake, D. N. Baker, C.-L. Huang, H. Spence, W. Kurth, C. Kletzing, and J. V. Rodriguez (2014), Competing source and loss mechanisms due to wave-particle interactions in earth's outer radiation belt during the 30 september to 3 october 2012 geomagnetic storm, *Journal of Geophysical Research: Space Physics*, *119*, 1960, doi:10.1002/2014JA019770.

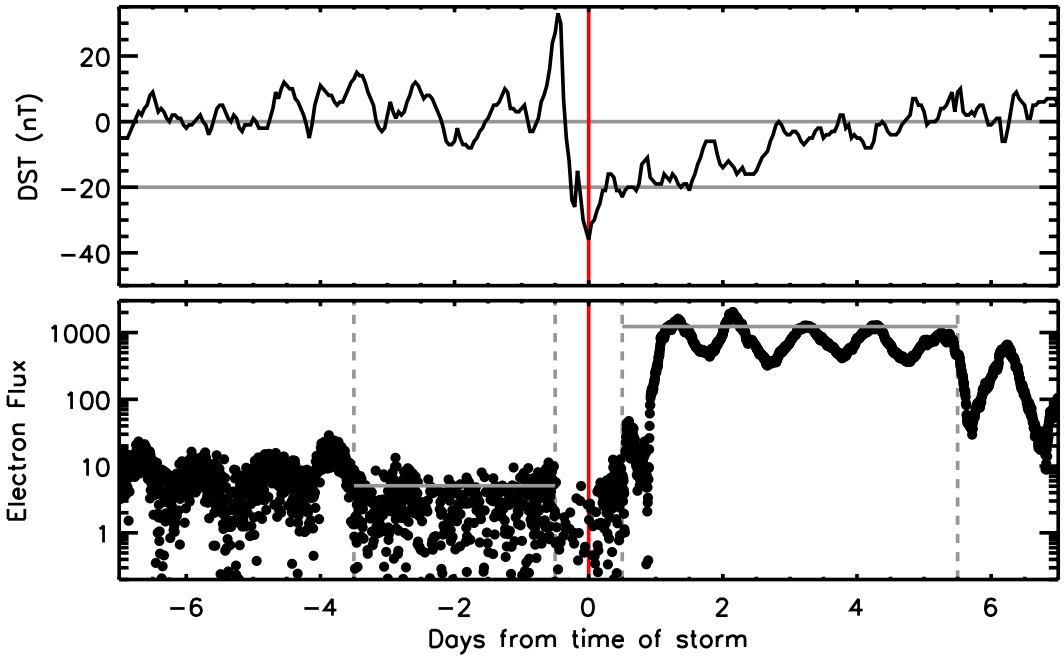

Figure 1. Example small storm during a BARREL test flight. Two weeks of data centered on the time of minimum Dst are plotted. The top panel shows Dst, with horizontal lines marking 0 nT and -20 nT as a guide. The bottom panel shows GOES-11 $>$ 2 MeV electron flux, with dashed vertical lines marking the pre- and post-storm periods and horizontal lines marking the 90th percentile flux level for each period. The red vertical line marks the time of the storm: 14 February 2009 1500UT. In the 12 hours prior to the storm, Dst dropped 69 nT to a minimum of -36 nT.

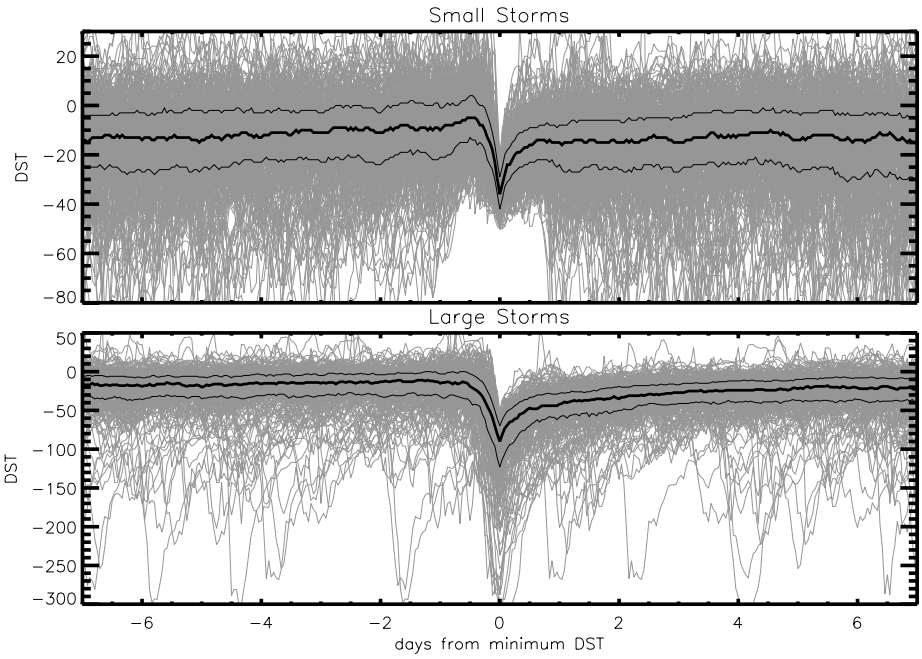

Figure 2. Superposed epoch of all small and large storms included in this study. Each plot shows the Dst signature a week before through a week after the time of minimum Dst. Median as well as upper and lower quartile levels for Dst are plotted in black lines.

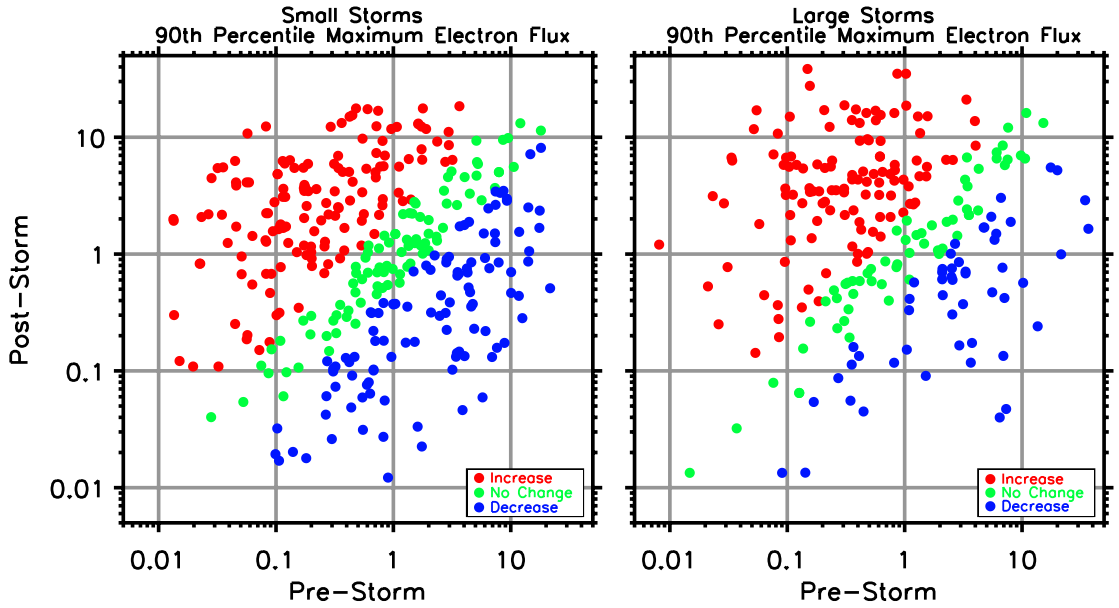

Figure 3. Distributions of Small Storms and Large Storms. 90th percentile maximum post-storm flux is on the vertical axes and that for pre-storm flux is on the horizontal axes. Each dot represents one storm and is colored to guide the eye to recognize those storms that resulted in an increase (red), no-change (green), or decrease (blue) in relativistic electron flux.

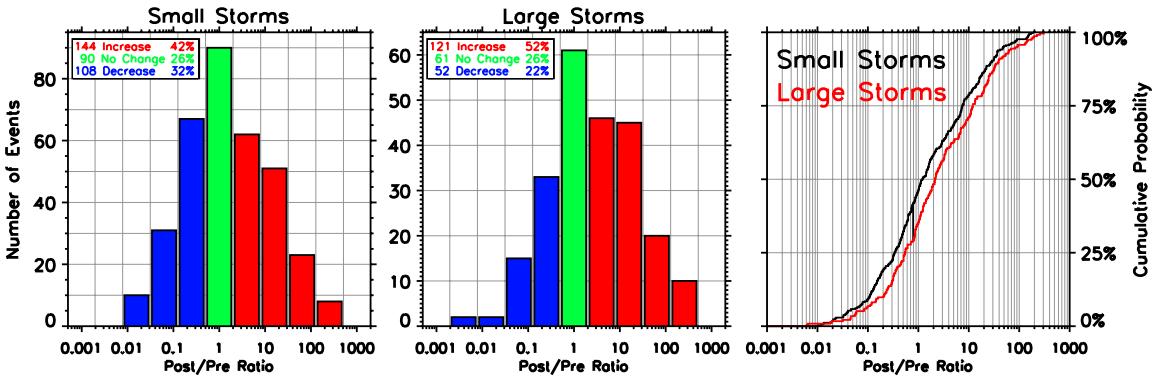

Figure 4. Histogram of the ratio of post/pre-storm 90th percentile maximum flux for a) Small and b) Large Storms. c) Cumulative probability distribution for small (black) and large (red) storms. The cumulative probability is the probability that a storm will result in a post/pre storm maximum flux ratio equal to or lesser than a given value. The dark vertical line represents the maximal difference between the two distributions (13%), which is used to determine the statistical likelihood the difference between the distributions is random ($< 2\%$).

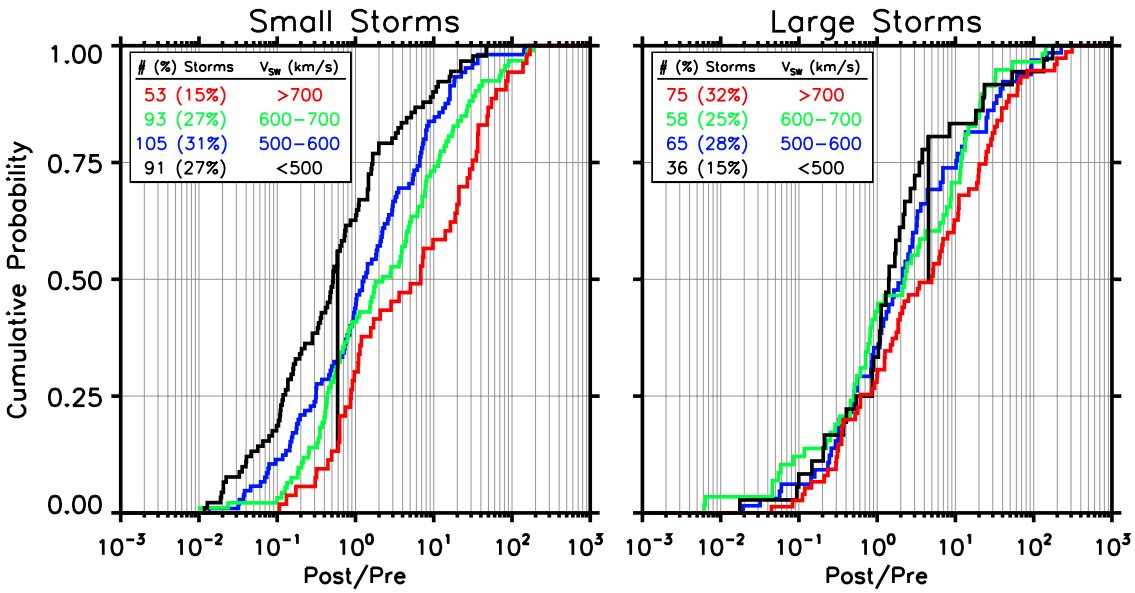

Figure 5. Cumulative probability distributions for small and large storms. For each plot, the set of storms is broken into four subgroups by maximum solar wind speed during the entire storm period.